

# A SUPERCONDUCTING BEARING SYSTEM USING HIGH $T_c$ SUPERCONDUCTORS

**Mochimitsu Komori**

Faculty of Computer Science and Systems Engineering,  
Kyushu Institute of Technology, Iizuka-city, Fukuoka, 820 Japan

**Akira Tsuruta, Satoru Fukata**

Faculty of Engineering, Kyushu University,  
Hakozaki, Higashi-ku, Fukuoka, 812 Japan

**Teruo Matsushita**

Faculty of Computer Science and Systems Engineering,  
Kyushu Institute of Technology, Iizuka-city, Fukuoka, 820 Japan

## ABSTRACT

To realize practical use of superconducting bearings, a superconducting bearing system using high  $T_c$  superconductors is newly constructed. The superconducting bearing system consists of two superconducting bearings and a rotor.

To evaluate the load capacity of the system, relationship between restoring force and displacement of the rotor in the radial direction is investigated. To construct a vibration model of the bearing system, responses for impulse forces given to the stationary rotor are measured. Spin-down tests are performed to evaluate dynamics of the rotor. The bearing system is very well self-centered in the speed range not more than 63,000 rpm. The displacements are smaller than 30  $\mu\text{m}$  except critical speeds.

Since the structure of the superconducting bearing system is very simple and easy to use, the bearing system is full of promise for industrial fields.

## I. INTRODUCTION

Recently high  $T_c$  (critical temperature) superconductors prepared by quench - melt - growth (QMG) process and other new methods show good properties such as strong pinning force for levitation applications.<sup>1</sup> Stable levitation systems with neither contacts can be realized using high  $T_c$  superconductors.<sup>2</sup> Among many applications of high  $T_c$  superconductors, efforts have been put into the development of superconducting bearing systems<sup>3,4</sup> based on the strong pinning force. Most of the bearing systems have a rotor with some permanent magnets for levitation and superconductors for support. These bearing systems are comparatively small for practical applications. Our group has reported a levitation mechanism using

high  $T_c$  superconductors and a set of alternating-polarity magnets<sup>5</sup> with a pole order of  $\cdots\text{NSSNNS}\cdots$ . As an application of this levitation mechanism, our group has succeeded in developing a superconducting bearing system for practical use.

This article describes dynamic characteristics of the stationary rotor and the rotating rotor, and dynamic modeling of the bearing system.

## II. BEARING SYSTEM

A prototype of superconducting bearing system for practical use was built as shown in Figures 1 and 2. Figures 1 and 2 indicate a schematic illustration and a photograph of the system, in which the rotor is incorporated into the bearing system. The bearing system consists of two superconducting bearings and a rotor. The rotor (24 mm $\phi$   $\times$  158 mm,  $3.21 \times 10^{-1}$  kg) is composed of aluminum shaft and two sets of four ring magnets. The sets of magnets have a pole order of NS-SN-NS-SN with an axial magnetization of  $B_r \approx 1.0$  T. A piece of the ring magnets is OD24  $\times$  ID8  $\times$  4.3 mm in sizes. The housings of the superconducting bearings are composed of cylindrical superconductors (OD45  $\times$  ID25.6  $\times$  16mm,  $J_c \approx 10^8$  A/m<sup>2</sup> at 1 T), which are shaped like a doughnut. The cylindrical superconductors are set in a tank filled with liquid nitrogen. Then, the rotor-bearing (tank) clearance is 0.5 mm. Four eddy current sensors of  $S_{11}$ ,  $S_{12}$ ,  $S_{21}$ , and  $S_{22}$  are installed in the system to measure the displacements of the rotor, as shown in Figures 1 and 2. During the experiments, the sensors are kept at room temperature.

Restoring forces and displacements of the rotor were measured by using a load cell and a mechanical stage, respectively. Further details of this are reported elsewhere.<sup>5</sup>

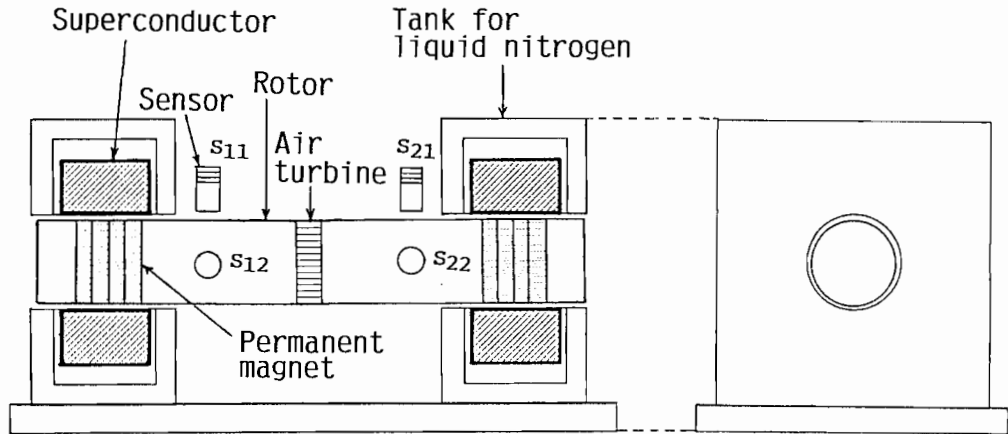


FIGURE 1: Schematic Illustration of the Superconducting Bearing System

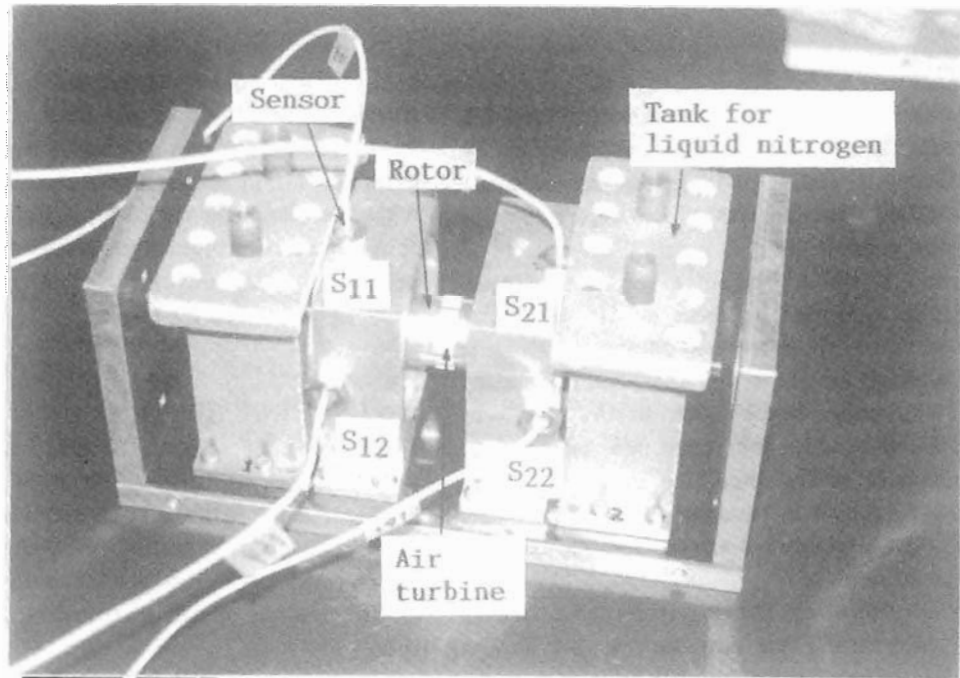


FIGURE 2: Photograph of the Superconducting Bearing System

For easy use in industrial fields, the superconductors of our bearing system are field-cooled in our experiments. Each end of the rotor is supported mechanically before the field-cooling process.

### III. STATIC CHARACTERISTICS

The relationship between the radial restoring force and the radial displacement in the superconducting bearings was investigated. The restoring force indicates the stability of the rotor in the radial direction. The result is shown in Figure 3. The displacement is varied within the range from  $-0.3$  to  $0.3$  mm. The change in the displacement is as follows:  $0 \rightarrow 0.1 \rightarrow -0.1 \rightarrow 0.2 \rightarrow -0.2 \rightarrow 0.3 \rightarrow -0.3 \rightarrow 0.3$  mm. The hysteretic relationship

between the restoring force and the displacement is observed. The relationship is approximately linear except the hysteresis in this displacement range. The gradient of the hysteresis loop for the displacement of  $0.3$  mm is  $4.0 \times 10^4$  N/m, and the hysteresis for the displacement of  $0$  mm is  $3.1$  N. In this case, the gradient corresponds to the static stiffness of the superconducting bearings. It is found that the static stiffness of the superconducting bearing is very small compared with that of active magnetic bearings.<sup>6</sup> The repulsion force for the displacement of  $0.3$  mm is about  $-11.6$  N. Since the mass of the rotor is  $3.21 \times 10^{-1}$  kg, it is large enough for the two bearings to support the rotor. During the rotation of the rotor, it seems that the restoring force is strong enough for the rotor to

restrain the motion in the axial direction. Therefore, this superconducting bearing is suitable to applications with small load capacity, such as cryogenic turbopumps and cryogenic gyroscopes.

Axial restoring forces for the axial displacements of the rotor were measured, which show the stability in the axial direction. The displacements of the rotor are changed similarly to the displacement pattern in Figure 3. Hysteresis loops in the restoring forces for axial displacements are observed. The results show that the relationship is approximately linear in this displacement range. The axial restoring forces in the superconducting bearings work as forces produced by thrust bearings to stop the motion in the axial direction. The relationship shown in Figure 4 shows similar relationship in Figure 3, except the force range.

The results of the force-displacement relationship in the radial direction and the axial direction indicate that the superconducting bearings work as not only radial bearings but also thrust bearings. Thus, our system offers us a remarkable advantage that only two superconducting bearings can replace ten electromagnets which make up five-axis control-type magnetic bearings.

#### IV. DYNAMIC MODEL OF THE ROTOR

To construct a vibration model of the superconducting

bearing system, responses for impulse forces given to the radial direction of the stationary rotor were measured. Then, the displacement of the rotor was detected by a FFT analyzer.

The experimental data are shown in Figure 5, where Figures 5 (a) and (b) show a free vibration curve and a power spectrum, respectively. As shown in Figure 5 (a), the amplitude of the curve seems to decrease exponentially. After the damped vibration, the amplitude returns to zero, that shows the position of the rotor is self-centered. The spectrum shown in Figure 5 (b) represents a remarkable peak at 92.5 Hz. Because analyses of bending vibration of the rotor show that the rotor is a rigid one, the vibration at the frequency of 92.5 Hz shown in Figure 5 (b) results from the stiffness of the superconducting bearings. Therefore, it is concluded that the superconducting bearing system is represented by a model with a mass, springs, and dampers.

From the previous discussion, we propose a dynamic model of the superconducting bearing system shown in Figure 6, where the rotor ( $m$ ) is supported by two superconducting bearings with dynamic stiffness ( $k_d$ ) and viscous damping coefficient ( $c$ ). Thus, the equation for the dynamic model shown in Figure 6 is written as

$$m\ddot{z} + 2c\dot{z} + 2k_d z = 0, \quad (1)$$

where  $z$  is the displacement of the rotor. Applying Equation (1) to our system, the dynamic stiffness and the damping coefficient are  $5.41 \times 10^4$  N/m and 27.2 Ns/m, respectively. The dynamic stiffness of  $5.41 \times 10^4$  N/m is a little larger than the static stiffness of  $4.0 \times 10^4$  N/m shown in Figure 3. The same results about the

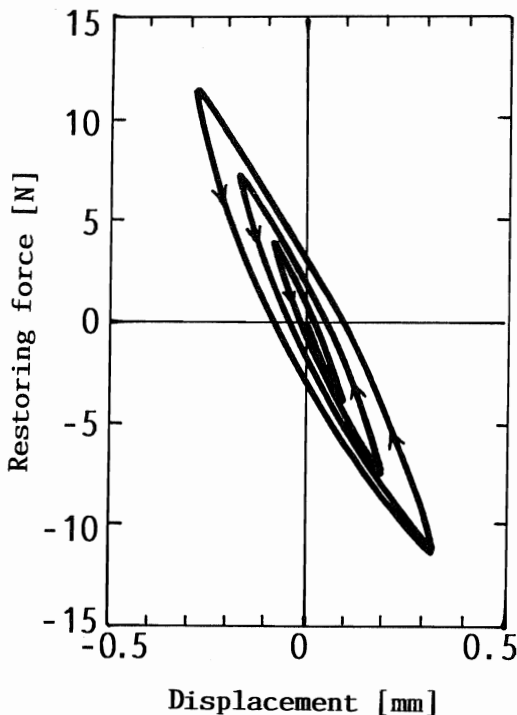


FIGURE 3: Relationship between the Radial Restoring Force and the Radial Displacement

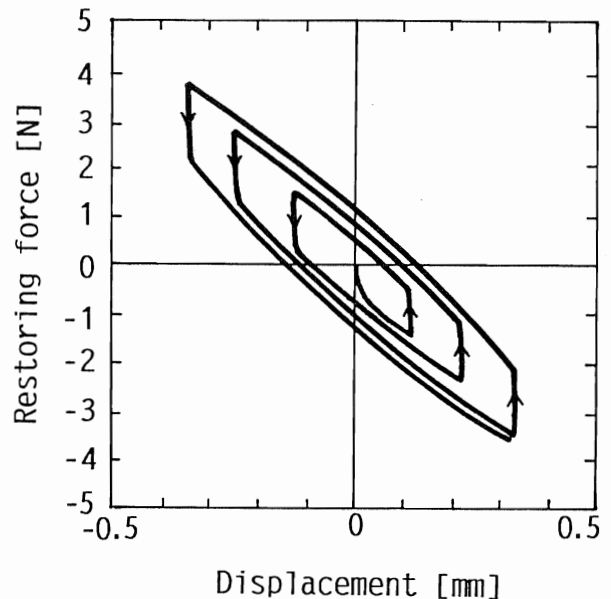


FIGURE 4: Relationship between the Axial Restoring Force and the Axial Displacement

bearing stiffness are reported elsewhere.<sup>7</sup>

Equation (1) is transformed into

$$\ddot{z} + 2\zeta\omega_n\dot{z} + \omega_n^2 z = 0, \quad (2)$$

where  $\omega_n = (2k_d/m)^{1/2}$  and  $\zeta = c(m\omega_n)^{-1}$  are natural angular frequency and damping ratio, respectively. Applying Equation (2) to our system, natural angular frequency  $\omega_n$  is 581 rad/s and damping ratio  $\zeta$  is  $7.30 \times 10^{-2}$ . Since the damping ratio of  $\zeta = 7.30 \times 10^{-2}$  is very small, the natural angular frequency of 581 rad/s is considered to be equal to the damped natural angular frequency, which shows 92.5 Hz (= 581 rad/s) in Figure 5 (b). Because the relationship between the natural angular frequency  $\omega_n$  and the damped natural angular frequency  $\omega_d$  is given by  $\omega_d = \omega_n(1-\zeta^2)^{1/2}$ .

### V. ROTATION CHARACTERISTICS

Rotation tests of the superconducting bearing system were performed, in order to investigate the rotation characteristics of the bearing system. Experimental setup for the rotation test was similar to the setup shown in Figures 1 and 2. After the compressed air was stopped to blow on the rotor turbine, the speed decay was measured as a function of time. The rotation speed was detected by a tachometer.

Figure 7 shows the relationship between the rotation speed and the time for an initial speed of 50,000 rpm. The rotation speed decreases monotonously with increasing time. The rotor continues rotating for more than 300 s. The rotor spun stably at the speed range not more than 50,000 rpm. The curve shows an exponential decay in the experiment.

In general, dynamic equation of the rotor is given by

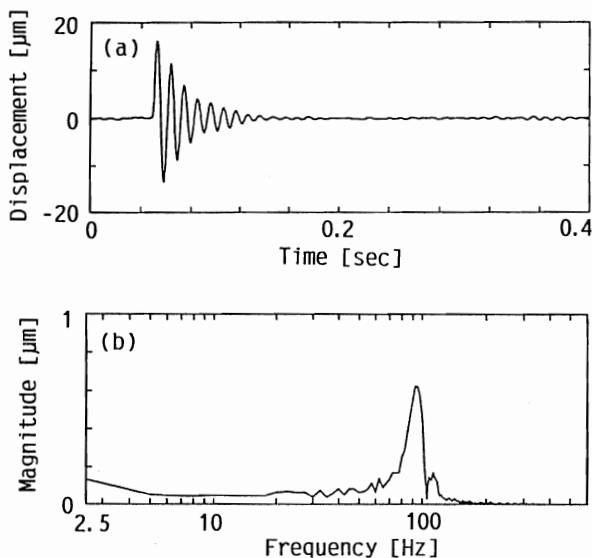


FIGURE 5: Impulse Responses of (a) Vibration Curve and (b) Power Spectrum of the Rotor

$$n = n_0 \exp(-t/T_0), \quad (3)$$

where  $n$ ,  $n_0$ , and  $T_0$  are a rotation speed, an initial rotation speed, and a time constant (=  $I/C_0$ ,  $I$ : axial moment of inertia,  $C_0$ : constant value), respectively. Applying Equation (3) to the curve in the speed range from 2,000 to 20,000 rpm shown in Figure 7, the exponential curve is represented by

$$n = 37,200 \exp(-t/68.3), \quad (4)$$

where the correlation coefficient is 0.999. The initial rotation speed (37,200 rpm) of Equation (4) is smaller than the actual initial speed of 50,000 rpm.

The displacements of the left superconducting bearing as a function of time were measured by using the displacement sensors  $S_{11}$  and  $S_{12}$ . The relationship between the displacement and the time for various rotation speeds of 40,000 and 63,000 rpm is shown in

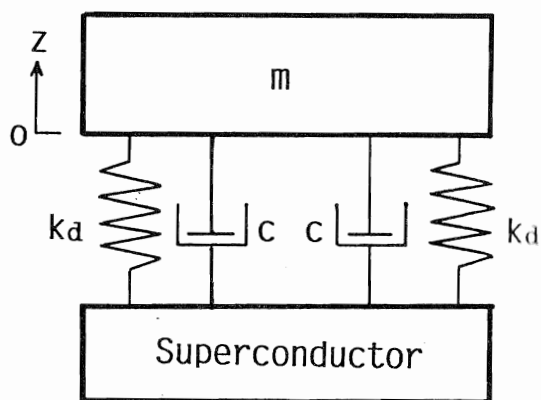


FIGURE 6: Dynamic Model of the Superconducting Bearing System

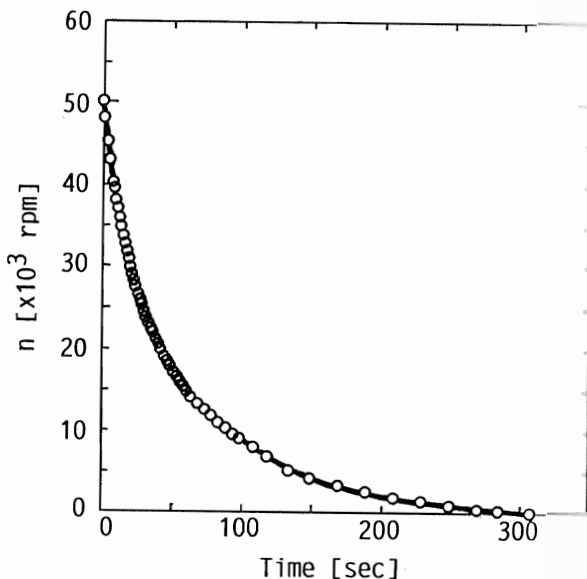


FIGURE 7: Relationship between the Rotation Speed and the Time

Figures 8 (a) and (b), respectively. Two displacement curves for sensors  $S_{11}$  and  $S_{12}$  are shown in each figure. The curves for sensors  $S_{11}$  and  $S_{12}$  are periodical, and resemble to each other except the phase delay. The periods of the curves indicate the time for a rotation of the rotor. As shown in Figure 8, the periods become short with increasing rotation speed. The displacements of the rotor are smaller than  $30 \mu\text{m}_p$ . The displacements of the left superconducting bearing shown in Figure 1 were almost similar to those of the right bearing, because the system is structurally symmetry from right to left as shown in Figures 1 and 2, and because the speed decay tests were performed without disturbance force.

The relationship between the displacement and the rotation speed is shown in Figure 9. Figure 9 shows that the superconducting bearing system has a critical speed in the neighborhood of 5,500 rpm. In the speed range not more than 50,000 rpm except around the critical speed, the displacements are smaller than  $30 \mu\text{m}_p$ . This is good for the superconducting bearing system to be applied to practical use, because the displacement of  $30 \mu\text{m}_p$  is negligible compared with the rotor-bearing (tank) clearance (0.5 mm) of the bearings. However, the displacement around the rotation speed of 5,500 rpm is approximately  $200 \mu\text{m}_p$ , which corresponds to the frequency of 92.5 Hz shown in Figure 5. This shows that the stiffness of the superconducting bearings is not large enough to restrain the displacement around the critical speed. Because the displacement of  $200 \mu\text{m}_p$  is smaller than the clearance of the bearings, there is no problem for the present.

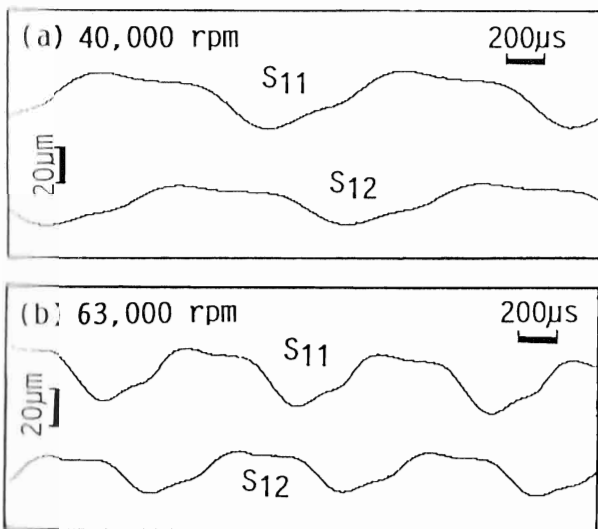


FIGURE 8: Displacements as a Function of Time Detected by  $S_{11}$  and  $S_{12}$

Overall drag torque acting on the rotor calculated as  $I d\omega/dt$  is evaluated using the data shown in Figure 7. Figure 10 shows the relationship between the drag torque and the rotation speed. The drag torque increases monotonously with increasing rotation speed. The drag torque at a speed of 15,000 rpm is about  $3 \times 10^{-4}$  Nm, which is considered to be small.

Using the experimental result shown in Figure 7, overall loss of the rotor was evaluated as shown in Figure 11. The overall loss  $\mathcal{K}$  is given by

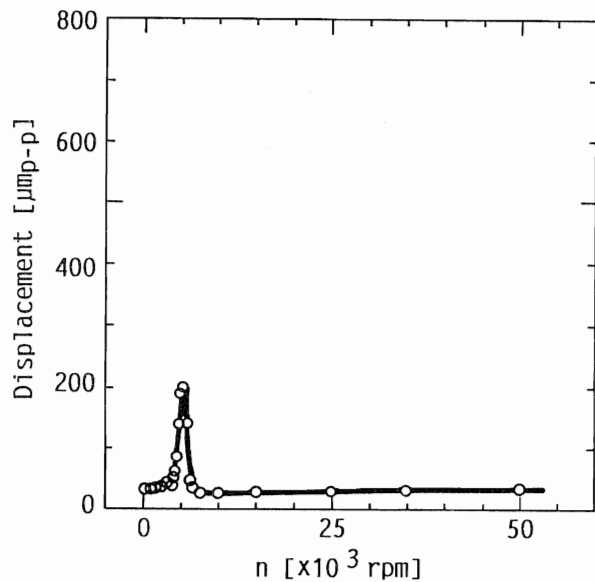


FIGURE 9: Relationship between the Displacement and the Rotation Speed

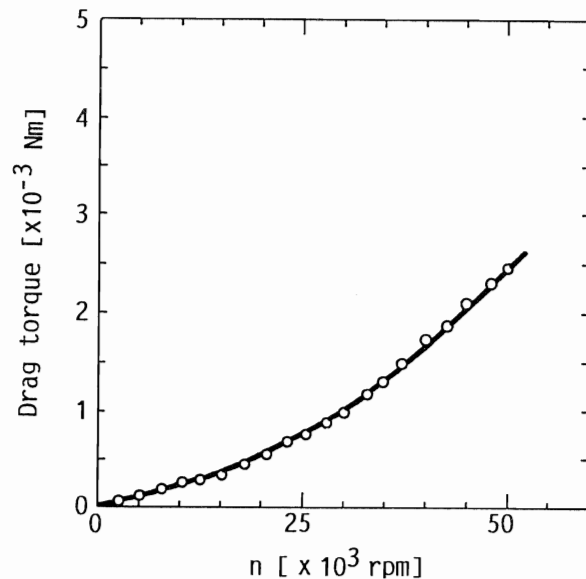


FIGURE 10: Relationship between the Overall Drag Torque and the Rotation Speed

$$\dot{W} = \frac{I\omega^2(t_n) - I\omega^2(t_{n+1})}{2\Delta t}, \quad (5)$$

where  $\omega(t_n)$  is angular frequency at a time  $t_n$  and  $\Delta t = t_n - t_{n+1}$ . The change in the loss becomes large with increasing rotation speed. At the rotation speed of 50,000 rpm, the loss is about 24 W. Because loss owing to the pinning force does not depend on the rotation speed, the rapid increase in the loss over the high speed range as shown in Figure 11 is considered to result from windage loss.

At present, the superconducting bearing system is not good enough for us to apply to industrial fields, because of the small load capacity. However, the superconducting bearing system proposed here has a very simple and easy-to-use structure. These indicate that the superconducting bearing system shows high potential for industrial application.

## VI. SUMMARY

A prototype of superconducting bearing system for practical use has been developed. From the experimental results, it is found that the superconducting bearings work as not only radial bearings but also thrust bearings, that characterizes our superconducting bearing system. The superconducting bearing system is represented by a dynamic model with a mass, two springs and two dampers. The rotor rotates stably at the speeds not more than 63,000 rpm. The bearing system has a critical speed around 5,500 rpm. In the speed range except around the critical speed, the displacements are smaller than  $30 \mu\text{m}$ . The overall drag torque and the overall loss of the rotor are evaluated. The results show that the bearing has high potential for practical use.

## ACKNOWLEDGMENTS

We would like to express our thanks to Dr. H. Hayashi, Dr. T. Toyoda, Mr. M. Ueno, Mr. M. Hara (Fujikoshi Corp.), Mr. S. Oshima, and Mr. T. Nakazeki (NTN Corp.) for their continuous support. The superconductors used in our experiments are supplied by Nippon Steel Corporation. This study is supported by the Iwatani Naoji Foundation's Research Grant.

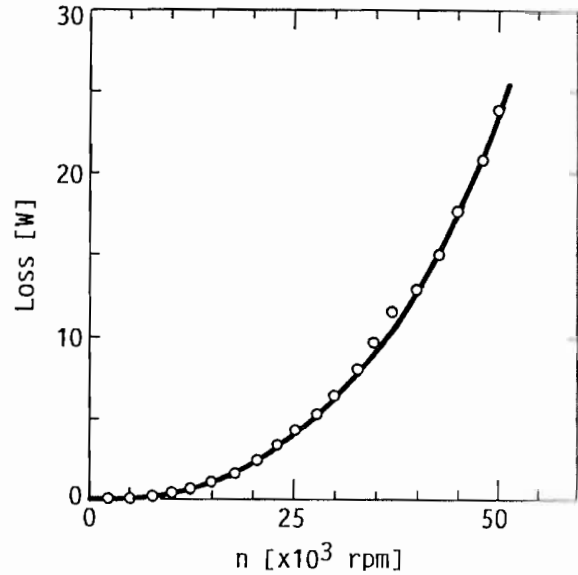


FIGURE 11: Relationship between the Overall Loss and the Rotation Speed

## REFERENCES

1. Murakami M., Morita M., Doi K., and Miyamoto K., A New Process with the Promise of High  $J_c$  in Oxide Superconductors, *Jpn. J. Appl. Phys.* 28, 1189 (1989).
2. Moon F. C., Yanoviak M. M., and Ware R., Hysteretic Levitation Forces in Superconducting Ceramics, *Appl. Phys. Lett.* 52, 1534 (1988).
3. Komori M. and Titamura K., Development of a Superconductive Levitational Mechanism and its Application to a Superconductive Radial Bearing, *Cryogenic Engineering*, 25, 411 (1990).
4. Moon F. C. and Chang P.-Z., High-speed Rotation of Magnets on High  $T_c$  Superconducting Bearings, *Appl. Phys. Lett.* 56, 397 (1990).
5. Komori M. and Titamura K., Static Levitation in a High- $T_c$  Superconductor Tile on Magnet Arrangements, *J. Appl. Phys.* 69, 7306 (1991).
6. *Magnetic Suspension Technology*, 1st Edn, Corona Publishing Co., Ltd. Tokyo (1993).
7. Komori M., Matsushita T., and Takeo M., Estimation of Hysteretic Levitation Pressure and Stiffness in High  $T_c$  Superconducting Bearings, *Cryogenics*, 33, 1058 (1993).